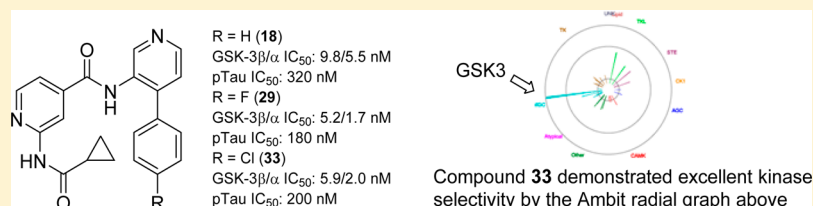


Discovery of Isonicotinamides as Highly Selective, Brain Penetrable, and Orally Active Glycogen Synthase Kinase-3 Inhibitors

Guanglin Luo,* Ling Chen, Catherine R. Burton, Hong Xiao, Prasanna Sivaprakasam, Carol M. Krause, Yang Cao, Nengyin Liu, Jonathan Lipky, Wendy J. Clarke, Kimberly Snow, Joseph Raybon, Vinod Arora, Matt Pokross, Kevin Kish, Hal A. Lewis, David R. Langley, John E. Macor, and Gene M. Dubowchik

Bristol-Myers Squibb Research & Development, Bristol-Myers Squibb Company, 5 Research Parkway, Wallingford, Connecticut 06492, United States

S Supporting Information



ABSTRACT: GSK-3 is a serine/threonine kinase that has numerous substrates. Many of these proteins are involved in the regulation of diverse cellular functions, including metabolism, differentiation, proliferation, and apoptosis. Inhibition of GSK-3 may be useful in treating a number of diseases including Alzheimer's disease (AD), type II diabetes, mood disorders, and some cancers, but the approach poses significant challenges. Here, we present a class of isonicotinamides that are potent, highly kinase-selective GSK-3 inhibitors, the members of which demonstrated oral activity in a triple-transgenic mouse model of AD. The remarkably high kinase selectivity and straightforward synthesis of these compounds bode well for their further exploration as tool compounds and therapeutics.

INTRODUCTION

Alzheimer's disease (AD) is the most common form of dementia and affects over 30 million people worldwide. An estimated 5.2 million Americans have AD, and it is the fifth leading cause of death in Americans age 65 or older.¹ AD is histopathologically defined by neuronal loss, the presence of intracellular neurofibrillary tangles (NFTs), the formation of extracellular senile plaques, and the occurrence of cerebral amyloid angiopathy.^{2,3} There is currently no disease-modifying treatment available. While extensive preclinical and clinical efforts have focused on beta-amyloid (Aβ)-related intervention, a related hypothesis is that hyperphosphorylation of tau protein leads to the destabilization of microtubules, which then aggregate to form NFTs.

Glycogen synthase kinase-3 (GSK-3) is a proline-directed serine/threonine kinase that is involved in the regulation of various physiological functions, such as metabolism, proliferation, and apoptosis, by carrying out the phosphorylation of multiple protein substrates.⁴ GSK-3 exists in two isoforms, GSK-3α (51 kDa) and GSK-3β (47 kDa), that share 84% overall identity and 98% identity within their respective catalytic domains.⁵ Both primary isoforms are ubiquitously expressed, with high levels observed in the brain.^{6,7} In most brain areas, GSK-3β is the predominant isoform.⁸ There is evidence to suggest that the GSK-3β isoform is the key kinase required for hyperphosphorylation of tau.^{9,10} However, some studies suggest that GSK-3α and GSK-3β share very similar, if

not entirely redundant, functions in a number of cellular processes.¹¹ GSK-3 is one of a small number of kinases that are constitutively active, and its activity generally results in a reduction of substrate function. The substrates on which it functions are numerous, with at least 50 being well-defined, but there are perhaps as many as 100 or more in total.¹² Given its central role in cellular differentiation and metabolism, acting on a large number of substrates, it is not surprising that GSK-3 is highly regulated. This is enforced by multiple mechanisms including substrate priming, activating phosphorylation, physical sequestration, and, most prominently, inhibitory phosphorylation. The activity of GSK-3β is significantly reduced by phosphorylation at Ser-9 in the N-terminal domain, most notably by protein kinase B (PKB or AKT).¹³ This inhibitory pathway has been proposed to result in neuroprotection, neurogenesis, and favorable outcomes following pharmacological treatment in various mood disorders. Hyperphosphorylation of tau by GSK-3 has been demonstrated both in cell culture and in *in vivo* studies.¹⁴ Hyperphosphorylated tau disengages from microtubules, resulting in destabilization of these filaments with concomitant negative effects on intracellular structures and transport mechanisms.¹⁵ In addition, the uncomplexed, hyperphosphorylated tau assembles into paired helical filaments (PHFs) that aggregate to produce the

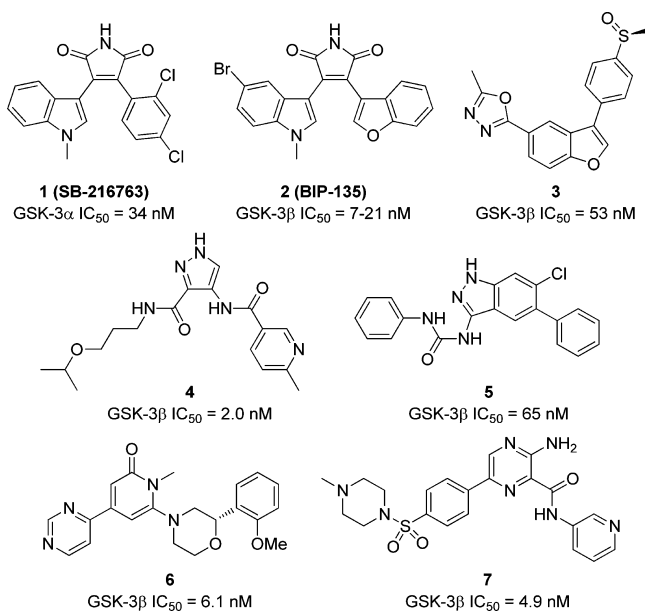
Received: October 5, 2015

stereotypic intracellular NFTs associated with AD.^{16–18} Other potential pathological consequences of overactivation of GSK-3 include neuroinflammation and apoptosis.^{19,20} Furthermore, GSK-3 has been demonstrated to be involved in mechanisms underlying memory and learning, and dysregulation of GSK-3 may explain some of the early cognitive deficits observed in AD.²¹ These results and observations suggest that inhibition of GSK-3 activity may be useful in the treatment of both the neuropathologic and symptomatic aspects of AD, as well as other neurodegenerative diseases. Recently, a non-ATP-competitive, irreversible GSK-3 inhibitor, Tideglusib, was tested in Phase II studies for AD.²²

GSK-3 inhibitors have also been studied as potential agents for the treatment of mood disorders²³ and metabolic diseases, such as type II diabetes²⁴ and bone density improvement.²⁵ Looming over these attractive opportunities for therapeutic intervention has been the perceived risk of hyperplasia resulting from interference in one of GSK-3's most prominent roles: phosphorylation of beta-catenin, leading to its eventual destruction in the proteasome.²⁶ However, over 50 years of clinical experience with lithium for treating bipolar disorder, which is now believed to work through GSK-3 inhibition, firmly establishes that these patients do not have increased cancer risks. Interestingly, several studies have shown an anticancer effect of GSK-3 inhibition, potentiating the effect of standard chemotherapy against a number of tumor types including pancreatic cancer and leukemias.²⁷ Initial phase I clinical data has recently been reported for a combination of Pemetrexed with a GSK-3 inhibitor, LY2090314.²⁸

Over the past 2 decades, a number of highly diverse classes of GSK-3 inhibitors have been discovered.^{29,30} Representative GSK-3 inhibitors are shown in Chart 1. SB-216763 (1) was an

Chart 1. Selected GSK-3 Inhibitors



early maleimide derivative that showed reduction of tau hyperphosphorylation in rat brain.³¹ Another maleimide derivative, BIP-135 (2), has recently shown activity in models of bipolar disorder and spinal muscular atrophy.³² Compound 3 showed a good brain/plasma (b/p) ratio and reduced tau hyperphosphorylation *in vivo*.^{33,34} Compound 4 was disclosed in 2009 as a potent and selective GSK-3 inhibitor that inhibited

tau phosphorylation in rat primary neuronal cells and mouse brain tissue.³⁵ Compounds 5–7 were recently disclosed to be brain-penetrable, but no efficacy data has so far been reported.^{36–38} Unfortunately, most GSK-3 inhibitors that are claimed to be selective have only been tested against a limited set of kinases. We believe that when targeting such a critical regulatory enzyme such as GSK-3, especially for a nononcology indication, kinase selectivity may be of paramount importance.

In a recent publication, we disclosed a series of GSK-3 inhibitors, exemplified by compound 8 (Figure 1).³⁹ Modeling

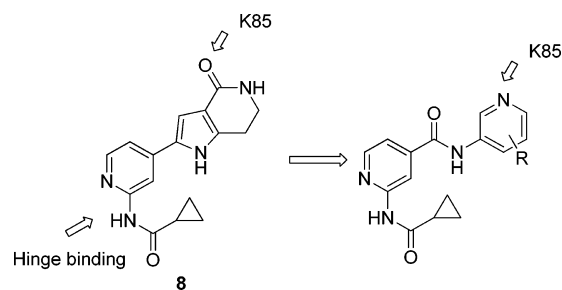


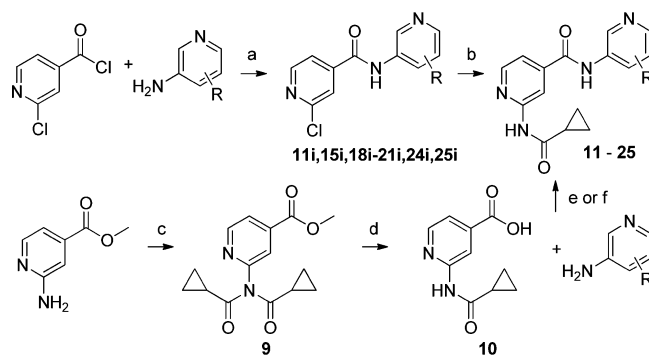
Figure 1. Design of the 3-pyridinyl isonicotinamides.

and X-ray structural studies showed that the left-side amino-pyridine bound to the hinge region of GSK-3 and the right-side amide carbonyl made a hydrogen bond with Lys-85 (K85). We were interested in replacing the lactam with pyridine, in which the pyridyl nitrogen would act as the H-bond acceptor, which might improve CNS penetration. To further simplify the synthesis and to give the rigid tricyclic scaffold a bit more flexibility, we also replaced the pyrrole portion with an amide group (Figure 1).

RESULTS AND DISCUSSION

The proposed isonicotinamides were synthesized by two general strategies (Scheme 1). In the initial approach, commercial isonicotinic acid dichloride was reacted with various 3-aminopyridines to generate the 2-chloroisonicotinamide intermediates, which were then subjected to Buchwald amidation without purification⁴⁰ to afford the desired products.

Scheme 1. Synthesis of 3-Pyridinyl Isonicotinamides^a



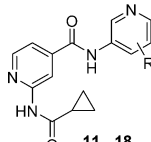
^aReagents and conditions: (a) CH₂Cl₂, *i*-Pr₂NEt, rt, 18 h; (b) cyclopropanecarboxamide, Pd(OAc)₂, K₂CO₃, Xantphos, dioxane, 150 °C, 2 h; (c) cyclopropanecarbonyl chloride (2.1 equiv), CH₂Cl₂, *i*-Pr₂NEt, 0 °C, 1 h (88%); (d) LiOH (4 equiv), THF–MeOH (10:1), rt, 18 h (79%); (e) 3-aminopyridine, HATU, DMF, rt (or 85 °C), *i*-Pr₂NEt, 18–48 h; (f) oxalyl chloride (1.2 equiv), DMF (cat.), rt, 30 min, then 3-aminopyridine, Et₃N, rt, 2 h.

For broader structural diversity or larger scale reactions, we developed a second, more convergent approach. Starting with 2-amino isonicotinic acid or its methyl ester, monoacylation of the amino group was not feasible (Figure 1). Instead, double acylation and the formation of the mixed anhydride always occurred. To solve this issue, methyl 2-amino isonicotinate was treated with excess acyl chloride (2.1 equiv) to afford the bis-acylated intermediate **9**. Subsequent treatment with 4 equiv of aqueous LiOH achieved complete conversion to the mono-acylated acid **10**, which upon neutralization with 4 equiv of aqueous HCl precipitated out as a white solid. The acid could directly react with many 3-aminopyridines under various amide formation conditions or be converted to the acyl chloride to react with more electron-deficient 3-aminopyridines.

Compounds were initially tested in GSK-3 β / α competition assays (GSK-3 β / α IC₅₀) with a fluorescently labeled small molecule at its K_d as well as in a cellular phosphorylated Tau (pTau) lowering assay (pTau IC₅₀).⁴¹ While a modest level of isoform selectivity was often seen with particular compounds in the enzyme assay, none of the compounds described herein could be described as truly selective in this respect. We also developed a similar assay in a vinblastine-resistant carcinoma (KBV) cell line that overexpresses human tau protein. Testing compounds with or without the P-glycoprotein (Pgp) inhibitor tariquidar allowed us to assess Pgp-related efflux. A resulting KBV ratio > 2 would suggest a low chance of significant brain penetration.

Data for an initial set of isonicotinamides is shown in Table 1. To our delight, the unsubstituted pyridine **11** showed good

Table 1. GSK-3 β / α Affinity and pTau for Compounds **11**–**18**



compd	R	GSK-3 β / α ^a IC ₅₀ (nM)	pTau IC ₅₀ (nM) ^b	KBV ratio
11	H	24(±3.0)/3.9	1400	0.4
12	2-F	37(±9.4)/34	1600	0.8
13	2-OH	490(±100)/210	10 000	0.7
14	2-CN	51(±18)/43		
15	4-OMe	3.4(±0.42)/4.5	240	1.4
16	4-Cl	11(±2.1)/4.5	260	1.2
17	4-CF ₃	19(±2.5)/6.3	960	1.3
18	4-Ph	9.8(±3.6)/5.5	320	1.3

^aValues are means of at least three experiments, but data for GSK-3 α was not repeated. ^bValues are means of at least two experiments.

enzymatic inhibition of GSK-3. Various substitutions at the 4-position were well-tolerated and usually improved enzyme inhibition and cell potency.

The proposed binding model for this series of compounds was confirmed by solving the X-ray co-crystal structures of select inhibitors with GSK-3 β .⁴² Figure 2 shows the details of key interactions observed with compound **15** binding in the active site, with respect to ADP.⁴³ The 2-aminopyridine makes hydrogen bonds with the hinge V135 backbone amide, and the 3-aminopyridine sp² nitrogen forms a key hydrogen bond with the K85 amine. Comparison with bound ADP suggested the 4-position of the 3-aminopyridine as a suitable vector to target

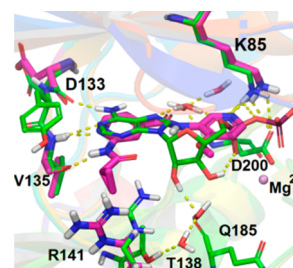
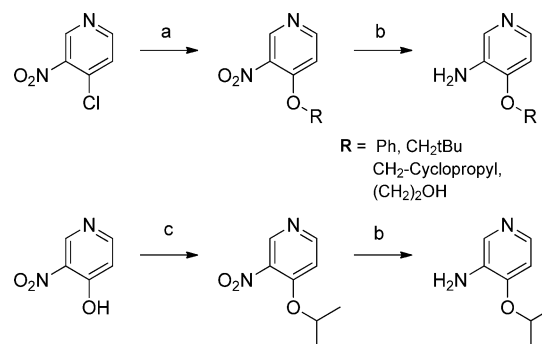


Figure 2. X-ray co-crystal structure of compound **15** in the kinase domain of GSK-3 β overlaid onto the X-ray structure of ADP bound GSK-3 β complex (PDB ID 1J1C).⁴³ The ligands are rendered as a stick model in green carbons for ADP and magenta carbons for compound **15**. Image was prepared using PyMOL.⁴⁴

the sugar pocket to optimize the potency and PK properties of this class of compounds. The bound structures also indicated that positions 4- and possibly 5- of the 3-aminopyridine should be more accessible for substitution than the more sterically crowded 2- and 6-positions. Two conserved structural water molecules observed in the back pocket were found to effectively bridge compound **15** through the central carbonyl oxygen.

The 4-methyl ether compound **15** (Table 1) significantly increased GSK-3 inhibition and cellular pTau lowering. We then further explored the SAR with regard to the alkoxy group. Various 4-alkoxy-3-pyridylamine intermediates were prepared as shown in Scheme 2. While direct substitution of the chloride

Scheme 2. Synthesis of 4-Alkoxy-pyridin-3-amines^a

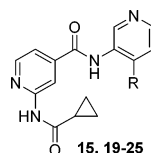


^aReagents and conditions: (a) alcohol/phenol, DMF, K₂CO₃, 65 °C, 18 h; (b) Pd/C/hydrogen (1 atm), MeOH; (c) *i*-PrOH, Ph₃P, DIAD, rt, 5 h.

by primary alcohols or phenol was straightforward, secondary alcohols such as *i*-PrOH failed. On the other hand, Mitsunobu coupling worked smoothly with 2-propanol followed by reduction of the nitro group via hydrogenation to afford the intermediate for compound **20**. The final compounds were prepared following the general sequence described in Scheme 1.

As shown in Table 2, all ether derivatives demonstrated single-digit nanomolar binding affinity toward GSK-3. In particular, the neopentyl ether **23** showed subnanomolar inhibition and very potent cellular pTau lowering (IC₅₀ = 36 nM). Unfortunately, the two most potent compounds in the cell assay, **23** and **24**, had poor metabolic stability, particularly in rodent liver microsomes (Table 2). The hydroxyethyl ether **25** had good potency and metabolic stability, but it had a high KBV efflux ratio (3.8). Data for compounds **15**, **19**, **21**, and **22** supported further profiling.

Table 2. Data for Compounds 15 and 19–25



compd	R	GSK-3 β / α^a IC ₅₀ (nM)	pTau IC ₅₀ ^b (nM)	KBV ratio	met. stab. (M/R/H) ^c
15	OMe	3.4(±0.42)/4.5	240	1.4	59/82/92
19	OCH ₂ CF ₃	2.5(±0.98)/2.2	260	1.4	57/90/100
20	O ⁱ Pr	1.9(±0.81)/1.4	1.5	0/23/65	
21	OEt	4.0(±1.3)/2.7	170	1.6	13/65/89
22	OPh	4.2(±1.1)/1.1	200	2.1	15/69/97
23	OCH ₂ <i>t</i> Bu	1.0(±1.1)/0.74	36	1.8	0/1/29
24	OCH ₂ -Cyclopropyl	2.4(±0.86)/1.8	65	1.2	0/35/81
25	O(CH ₂) ₂ OH	4.2(±0.55)/3.2	270	3.8	50/80/88

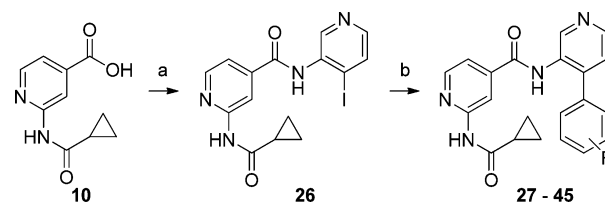
^aValues are means of at least three experiments, but data for GSK-3 α was not repeated. ^bValues are means of at least two experiments.

^cValues are percentage remaining after 10 min with 0.5 μ M compound incubated in liver microsomes.

Since we were targeting some level of chronic inhibition of GSK-3, a master regulatory kinase, we considered a high degree of selectivity over off-target kinases to be highly desirable. For broad kinase screening, we utilized the Ambit panel of almost 400 kinases, where selected compounds were tested at 1 μ M.⁴⁵ As represented by the Ambit radial graphs shown in Figure 3,⁴¹ the pyrrolopyridinone 8 had very poor kinase selectivity, whereas the isonicotinamide methyl ether 15 was dramatically improved. These results were in agreement with IC₅₀ data from a smaller in-house panel of 30 kinases, which were generally greater than the concentrations tested at 2 or 50 μ M.⁴⁶

We decided to explore SAR around the phenyl group of compound 18. These analogues were prepared by Suzuki coupling with a common iodide intermediate 26 (Scheme 3), which was prepared from the carboxylic acid 10.

As shown in Table 3, a single fluorine was well-tolerated at the 4-position (29) but less so at the 2- and 3-positions (27 and 28). Other 4-substituted analogues (29–36) showed good enzyme and cell potencies with the exception of the *t*-butyl

Scheme 3. Synthesis of 27–45^a

^aReagents and conditions: (a) oxalyl chloride (1.2 equiv), DMF (cat.), 0 °C, 2 h, then 4-iodopyridin-3-amine, Et₃N, 0 °C to rt; (b) aryl boronic acid, Na₂CO₃ (2.0 M), Pd(PPh₃)₄, dioxane, 110 °C (microwave), 30 min.

compound (36). Generally poor rodent metabolic stability was seen for most examples, but several showed promising human stability. Nitrile 32 looked good with respect to metabolic stability; however, as with other examples such as 25 in which polarity was introduced in this region, it was a strong Pgp substrate. The 2-CF₃ and 2-Cl derivatives, as well as various 2,4-disubstituted analogues (37–43), showed improved GSK-3 activities but had very poor metabolic stability. No advantage was seen with 2,5- or 2,3-difluoro substitution (44 and 45).

Ambit screening with almost 400 kinases of the phenyl compounds, 18, 29, and 33, showed them to have excellent kinase selectivity (Figure 4).⁴⁷ These compounds showed appreciable inhibitory activity, at least in these assays, only to the two GSK-3 isoforms.⁴⁷

It appears that a combination of the central amide linker, which participates in water-mediated hydrogen bonding in the rear of the ATP pocket, and the strongly tilted 4-phenyl group occupying the large sugar pocket in GSK-3 β are primarily responsible for the high degree of kinase selectivity observed. Notably, the back pocket region of kinases varies in size and shape partly due to the nonconserved nature of the gate keeper residue. Also, the hydrophilic sugar pocket has been used to achieve selectivity,⁴⁸ as the residues that make up this pocket are also not highly conserved. A surface representation of 18 bound in the GSK-3 β kinase domain (2.9 Å) is shown in Figure 5. The modeled water-mediated hydrogen bond network proposed for this class of compounds is also shown in the inset.

Consistent with their favorable cellular KBV ratios, compounds 18 and 33, had very good Caco-2 permeabilities

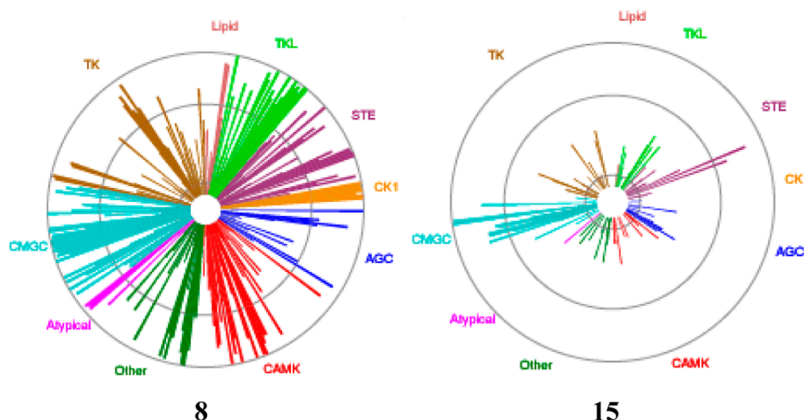
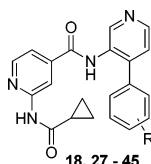


Figure 3. Ambit radial graphs of compounds 8³⁹ and 15. This is a single-point assay panel with a control for each kinase. Each line represents remaining activity of a single kinase in the presence of 1 μ M test compound. Starting from the center, the circles denote 83, 33, and 0% of control binding remaining.⁴⁵ The kinases are grouped into families differing by line color. As shown for 15, the two teal lines at nearly 0% represent GSK-3 α and β .

Table 3. Data for Compounds 18 and 27–45



compd	R	GSK-3 β / α^a IC ₅₀ (nM)	pTau IC ₅₀ (nM) ^b	KBV ratio	met. stab. (M/R/H) ^c
18	H	9.8(±3.6)/5.5	320	1.3	50/88/93
27	2-F	13(±4.2)/3.3	290	2.0	33/85/86
28	3-F	16(±11)/–	480	1.5	40/76/75
29	4-F	5.2(±2.2)/1.7	180	1.3	61/85/72
30	4-OMe	2.1(±0.95)/0.45	77	1.8	14/64/51
31	4-OCF ₃	11(±3.5)/6.9	270	1.3	36/74/44
32	4-CN	4.7(±1.3)/1.9	96	4.0	69/90/88
33	4-Cl	5.9(±2.7)/2.0	200	1.2	64/89/76
34	4-OCHF ₂	5.9(±2.3)/3.1	180	1.1	39/75/0
35	4-Me	4.7(±1.6)/1.1	120	0.83	3/33/25
36	4- <i>t</i> Bu	19(±8.9)/19	800	1.3	0/15/1
37	2-CF ₃	2.0(±0.69)/0.66	28	1.4	0/4/7
38	2-Cl	3.7(±1.1)/0.88	61	1.1	1/27/16
39	2,4-F ₂	1.9(±1.2)/0.34	62	0.83	48/87/66
40	2,4-Cl ₂	2.2(±1.2)/2.1	47	2.1	8/41/22
41	2-Cl-4-F	1.2(±1.1)/0.28	29	1.0	2/32/34
42	2-CF ₃ -4-F	0.87(±1.2)/0.17	14	1.2	0/11/13
43	2-F-4-Cl	2.8(±0.91)/1.2	75	0.91	36/80/63
44	2,5-F ₂	20(±5.4)/15	770	1.7	30/63/82
45	2,3-F ₂	10(±4.8)/6.4	230	1.1	29/62/52

^aValues are means of at least three experiments, but data for GSK-3 α was not repeated. ^bValues are means of at least two experiments. ^cValues are percentage remaining after 10 min with 0.5 μ M compound incubated in liver microsomes.

with no observed active efflux (Table 4). In addition, both compounds showed excellent inherent bilayer permeability in the PAMPA assay.

We tested selected compounds in a triple-transgenic mouse AD model.⁴⁹ These mice show elevated pTau levels and develop mild functional deficits, plaques, and tangles that are hallmarks of AD. It is important to note that, when tested, these compounds showed very high clearance in mice (for compound 29, Cl = 133 mL/min/kg, or >100% of hepatic blood flow), primarily due to facile hydrolysis of the pyridyl-2-aminocarboxamide and pyridyl N-oxidation of the 3-aminopyridine. When incubated in mouse serum at 37 °C, 24% amide cleavage from compound 18 was observed over 3 h, whereas only trace levels were detected in human serum. No degradants from

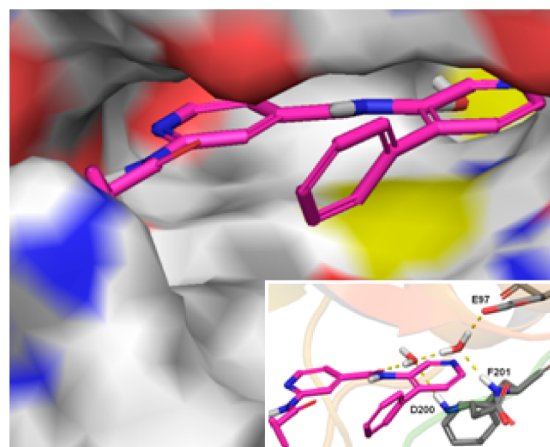


Figure 5. Surface representation of compound 18 bound to the ATP-binding site of GSK-3 β showing the 4-phenyl group of the 3-aminopyridine occupying the sugar pocket. The two conserved structural water molecules that were not detected in the X-ray structure of GSK-3 β –compound 18 complex most likely due to the low resolution (3.0 Å) were modeled and are shown in the inset.

Table 4. Permeability Data for Compounds 18 and 33

compd	Caco-2 P_c A–B, nm/s	Caco-2 P_c B–A, nm/s	efflux ratio	PAMPA P_c (pH 7.4), nm/s	PAMPA P_c (pH 5.5), nm/s
18	319	301	0.95	483	526
33	354	279	0.80	1260	904

cleavage of the core amide were seen. Less rapid *in vivo* clearance was seen for compound 18 in rat (24 mL/min/kg) and dog (9.6 mL/min/kg). We believe that this rapid clearance in mice resulted in a high degree of variability seen in plasma and brain exposures of compounds dosed po in these studies⁵⁰ and limits the extent of PK/PD interpretation possible in this species. In addition, compound 18 had IC₅₀'s all higher than 20 μ M in the CYP panel and higher than 80 μ M in the hERG flux assay.

Compound 18 showed significant activity at 30 mg/kg po in two independent studies in this model (results for one study are shown in Figure 6). The effect was comparable to the maximal pTau reduction achievable with LiCl at its MTD (250 mg/kg) and persisted to 24 h (pTau levels shown are normalized to total Tau). It is important to note that the maximal pTau reduction achievable with GSK-3 inhibition in this model is 50%, presumably due to the action of other kinases. Only a trend toward activity was seen at 3 and 10 mg/kg. Similar results were obtained with compound 29 (data not

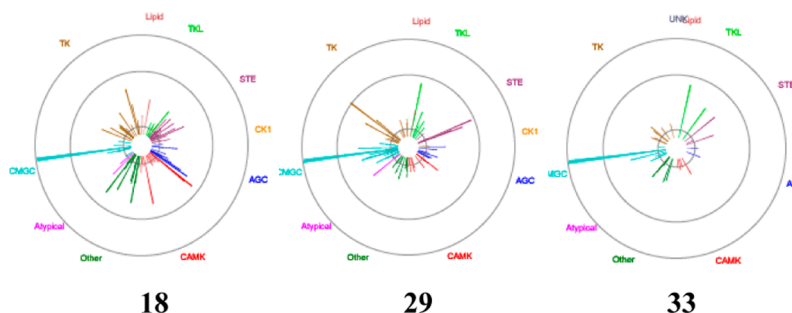


Figure 4. Ambit radial graphs for compounds 18, 29, and 33.

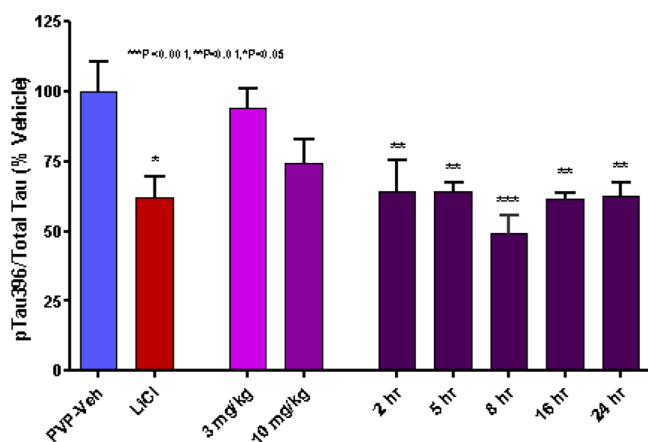


Figure 6. Dose–response (3, 10 mg/kg at 5 h) and time course (30 mg/kg) of **18** in the triple-transgenic mouse AD model.⁴⁹ The blue bar represents vehicle only, and the red bar shows maximum pTau reduction by LiCl (250 mg/kg ip).

shown). In the same model, the alkoxyphenyl compounds, **15**, **19**, **21**, and **22**, were inactive at 30 mg/kg po. Subsequent studies showed **18** to have somewhat robust but variable brain exposures (440 ± 362 nM at 2 h) and a b/p ratio of 0.2–0.3.⁵⁰ The alkoxy analogues, on the other hand, demonstrated poor oral exposures and no detectable brain levels (e.g., compound **21** had plasma exposure of 47 nM at 30 mg/kg, po).

In two separate time-course/dose–response studies, compound **33** showed significant activity at 10 and 30 mg/kg, po, at various time points (Figure 7). At 1 and 3 mg/kg, significant

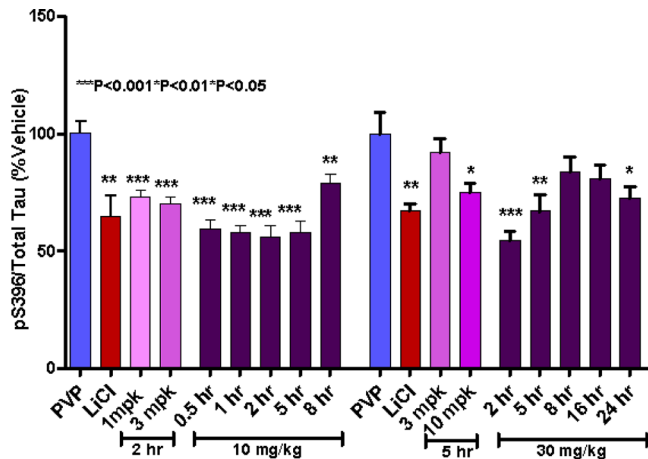


Figure 7. Dose–response of **33** at 1, 3, 10, and 30 mg/kg po and time course at both 10 and 30 mg/kg po in the mouse AD model.

activity was also seen at 2 h. Brain-to-plasma levels were higher in comparison with those for **18** (≥ 0.5), but interanimal variability was large, complicating interpretation.⁵⁰

CONCLUSIONS

In summary, we have discovered a novel class of potent GSK-3 inhibitors such as **18**, **29**, and **33** that show remarkable kinase selectivity in broad panel screening. Despite high *in vivo* clearance, these compounds showed good *in vivo* activity, lowering pTau levels in a triple-transgenic AD mouse model. With their very high level of kinase selectivity, radiolabeled versions of these molecules would be useful tools in further

studies. These and further SAR studies around this chemotype will be reported in due course.

EXPERIMENTAL SECTION

General Chemistry Details. All commercially available reagents and solvents were used without further purification unless otherwise stated. All reactions were carried out under an inert atmosphere of dry nitrogen in oven- or flame-dried glassware unless otherwise stated. Flash column chromatography was performed using 40–60 μ m silica gel 60 (EMD Chemicals, Inc.) as the stationary phase or prepacked columns from ISCO Inc., Biotage, or Thomson Instrument Co. ¹H NMR spectra were recorded on a Bruker 400 or 500 MHz machine with tetramethylsilane or residual protiated solvent used as a reference. ¹³C NMR were recorded on a Bruker DRX-500 instrument operating at 125 MHz with residual ¹²C solvent used as a reference. Low-resolution mass spectra were recorded using a Waters Micromass ZQ with electrospray ionization. High-resolution mass spectra were recorded using a Waters Micromass LCT time-of-flight mass spectrometer with electrospray ionization. The purity of all compounds was determined by either liquid chromatography–mass spectrometry (LCMS) or analytical HPLC and was confirmed to be greater than 95%.

2-Chloro-N-(pyridin-3-yl)isonicotinamide (11i). In a 10 mL round-bottomed flask was dissolved 2-chloroisonicotinoyl chloride (227.3 mg, 1.291 mmol) in methylene chloride to give a colorless solution. Pyridin-3-amine (134 mg, 1.42 mmol) was added, and a precipitate formed. Hunig's base (0.248 mL, 1.421 mmol) was added, and all solids were dissolved. The mixture was stirred at rt for 18 h. The mixture was purified by flash column chromatography using silica gel and eluting with a gradient up to 8% methanol/methylene chloride, affording the desired product (248.4 mg, 82%) as a white solid: MS (ESI) (*m/z*): 234 (*M* + *H*)⁺; ¹H NMR (400 MHz, CDCl₃) δ 8.73 (d, *J* = 2.5 Hz, 1H), 8.62 (dd, *J* = 5.1, 0.6 Hz, 1H), 8.47 (dd, *J* = 4.8, 1.4 Hz, 1H), 8.30 (d, *J* = 7.5 Hz, 1H), 8.20 (s, 1H), 7.85–7.79 (m, 1H), 7.69 (dd, *J* = 5.1, 1.5 Hz, 1H), 7.40 (dd, *J* = 8.3, 4.8 Hz, 1H).

2-Chloro-N-(4-methoxypyridin-3-yl)isonicotinamide (15i). MS (ESI) (*m/z*): 264 (*M* + *H*)⁺; ¹H NMR (400 MHz, CDCl₃) δ 9.41 (s, 1H), 8.58 (s, 1H), 8.52 (d, *J* = 5.1 Hz, 1H), 8.29 (d, *J* = 5.6 Hz, 1H), 7.75 (s, 1H), 7.63 (dd, *J* = 5.1, 1.4 Hz, 1H), 6.86 (d, *J* = 5.6 Hz, 1H), 3.97 (s, 3H).

2-Chloro-N-(4-phenylpyridin-3-yl)isonicotinamide (18i). MS (ESI) (*m/z*): 310 (*M* + *H*)⁺.

2-Chloro-N-(4-(2,2,2-trifluoroethoxy)pyridin-3-yl)isonicotinamide (19i). MS (ESI) (*m/z*): 332 (*M* + *H*)⁺.

2-Chloro-N-(4-isopropoxy)pyridin-3-yl)isonicotinamide (20i). MS (ESI) (*m/z*): 292 (*M* + *H*)⁺; ¹H NMR (400 MHz, CDCl₃) δ 9.33 (s, 1H), 8.64 (s, 1H), 8.47 (dd, *J* = 5.1, 0.5 Hz, 1H), 8.20 (d, *J* = 5.6 Hz, 1H), 7.70 (d, *J* = 0.7 Hz, 1H), 7.56 (dd, *J* = 5.1, 1.5 Hz, 1H), 6.80 (d, *J* = 5.7 Hz, 1H), 4.70 (hept, *J* = 6.1 Hz, 1H), 1.37 (d, *J* = 6.1 Hz, 6H).

2-Chloro-N-(4-ethoxy)pyridin-3-yl)isonicotinamide (21i). MS (ESI) (*m/z*): 278 (*M* + *H*)⁺; ¹H NMR (400 MHz, CDCl₃) δ 9.51 (s, 1H), 8.61–8.55 (m, 1H), 8.41 (br. s., 1H), 8.32 (d, *J* = 5.5 Hz, 1H), 7.80–7.75 (m, 1H), 7.62 (dd, *J* = 5.0, 1.5 Hz, 1H), 6.86 (d, *J* = 5.5 Hz, 1H), 4.25 (q, *J* = 7.0 Hz, 2H), 1.53 (t, *J* = 7.0 Hz, 3H).

2-Chloro-N-(4-(cyclopropylmethoxy)pyridin-3-yl)isonicotinamide (24i). MS (ESI) (*m/z*): 304 (*M* + *H*)⁺; ¹H NMR (400 MHz, CDCl₃) δ 9.39 (s, 1H), 8.65 (s, 1H), 8.51 (dd, *J* = 5.1, 0.5 Hz, 1H), 8.24 (d, *J* = 5.6 Hz, 1H), 7.74 (d, *J* = 0.7 Hz, 1H), 7.60 (dd, *J* = 5.1, 1.5 Hz, 1H), 6.80 (d, *J* = 5.6 Hz, 1H), 3.96 (d, *J* = 7.1 Hz, 2H), 1.38–1.23 (m, 1H), 0.72–0.63 (m, 2H), 0.40–0.33 (m, 2H).

2-Chloro-N-(4-(2-hydroxyethoxy)pyridin-3-yl)isonicotinamide (25i). MS (ESI) (*m/z*): 294 (*M* + *H*)⁺; ¹H NMR (400 MHz, MeOD) δ 9.06 (s, 1H), 8.57 (dd, *J* = 5.1, 0.6 Hz, 1H), 8.29 (d, *J* = 5.8 Hz, 1H), 7.95 (d, *J* = 0.7 Hz, 1H), 7.84 (dd, *J* = 5.2, 1.5 Hz, 1H), 7.15 (d, *J* = 5.8 Hz, 1H), 4.30–4.24 (m, 2H), 4.01–3.94 (m, 2H).

2-(Cyclopropanecarboxamido)-N-(pyridin-3-yl)isonicotinamide (11). To a 5 mL microwave tube under a nitrogen atmosphere were added **11i** (50.5 mg, 0.216 mmol), cyclopropanecarboxamide (55.2 mg, 0.648 mmol), and potassium carbonate (44.8 mg, 0.324 mmol) in dioxane (2 mL) (degassed) to give a colorless suspension. Pd(OAc)₂

(7.28 mg, 0.032 mmol) and Xantphos (37.5 mg, 0.065 mmol) were added. The vial was sealed and heated at 150 °C for 2 h. Volatile components were removed *in vacuo*. The residue was suspended in 3 mL of dimethylformamide and filtered. The solution was purified by prep-HPLC to afford the desired product (5 mg, 8%): MS (ESI) (*m/z*): 283 (*M* + *H*)⁺; ¹H NMR (500 MHz, DMSO-*d*₆) δ 11.06 (s, 1H), 10.74 (s, 1H), 8.92 (d, *J* = 2.4 Hz, 1H), 8.55 (s, 1H), 8.53 (d, *J* = 5.0 Hz, 1H), 8.36 (dd, *J* = 4.7, 1.5 Hz, 1H), 8.19 (ddd, *J* = 8.3, 2.5, 1.5 Hz, 1H), 7.57 (dd, *J* = 5.1, 1.5 Hz, 1H), 7.43 (ddd, *J* = 8.3, 4.7, 0.6 Hz, 1H), 2.14–1.99 (m, 1H), 0.93–0.81 (m, 4H).

2-(Cyclopropanecarboxamido)-N-(4-methoxypyridin-3-yl)-isonicotinamide (15). MS (ESI) (*m/z*): 313 (*M* + *H*)⁺; ¹H NMR (500 MHz, DMSO-*d*₆) δ 11.02 (s, 1H), 10.07 (s, 1H), 8.57 (s, 1H), 8.54 (s, 1H), 8.50 (d, *J* = 5.0 Hz, 1H), 8.38 (d, *J* = 5.6 Hz, 1H), 7.57 (d, *J* = 4.5 Hz, 1H), 7.19 (d, *J* = 5.7 Hz, 1H), 3.90 (s, 3H), 2.05 (tt, *J* = 6.9, 5.5 Hz, 1H), 0.92–0.80 (m, 4H).

2-(Cyclopropanecarboxamido)-N-(4-phenylpyridin-3-yl)-isonicotinamide (18). HRMS (ESI) (*m/z*): calcd for C₂₁H₁₉O₂N₄, 359.1503 (*M* + *H*)⁺; found, 359.1492; ¹H NMR (500 MHz, DMSO-*d*₆) δ 11.00 (s, 1H), 10.46 (s, 1H), 8.63 (s, 1H), 8.58 (d, *J* = 5.0 Hz, 1H), 8.46 (d, *J* = 4.5 Hz, 2H), 7.55–7.48 (m, 3H), 7.48–7.43 (m, 2H), 7.40 (tt, *J* = 6.2, 1.4 Hz, 2H), 2.04 (tt, *J* = 7.1, 5.3 Hz, 1H), 0.90–0.80 (m, 4H).

2-(Cyclopropanecarboxamido)-N-(4-(2,2,2-trifluoroethoxy)-pyridin-3-yl)isonicotinamide (19). MS (ESI) (*m/z*): 381 (*M* + *H*)⁺; ¹H NMR (500 MHz, MeOD) δ 11.83 (s, 1H), 11.01 (s, 1H), 9.34 (s, 2H), 9.32 (d, *J* = 5.2 Hz, 1H), 9.25 (d, *J* = 5.7 Hz, 1H), 8.33 (d, *J* = 4.3 Hz, 1H), 8.13 (d, *J* = 5.7 Hz, 1H), 5.76 (q, *J* = 8.7 Hz, 2H), 2.85 (dq, *J* = 6.6, 5.7 Hz, 1H), 1.69–1.64 (m, 4H).

2-(Cyclopropanecarboxamido)-N-(4-isopropoxy)pyridin-3-yl)-isonicotinamide (20). MS (ESI) (*m/z*): 341 (*M* + *H*)⁺; ¹H NMR (500 MHz, DMSO-*d*₆) δ 11.03 (s, 1H), 9.86 (s, 1H), 8.60 (s, 1H), 8.55 (s, 1H), 8.51 (d, *J* = 5.1 Hz, 1H), 8.32 (d, *J* = 5.6 Hz, 1H), 7.54 (s, 1H), 7.18 (d, *J* = 5.8 Hz, 1H), 4.80 (dt, *J* = 12.1, 6.0 Hz, 1H), 2.10–2.01 (m, 1H), 1.31 (d, *J* = 6.0 Hz, 6H), 0.90–0.84 (m, 4H).

2-(Cyclopropanecarboxamido)-N-(4-ethoxypyridin-3-yl)-isonicotinamide (21). MS (ESI) (*m/z*): 327 (*M* + *H*)⁺; ¹H NMR (400 MHz, CDCl₃) δ 9.58 (s, 1H), 8.70 (s, 1H), 8.50–8.41 (m, 3H), 8.35 (d, *J* = 5.5 Hz, 1H), 7.59 (dd, *J* = 5.0, 1.5 Hz, 1H), 6.87 (d, *J* = 5.5 Hz, 1H), 4.24 (q, *J* = 7.0 Hz, 2H), 1.67–1.60 (m, 1H), 1.59–1.54 (m, 3H), 1.17–1.12 (m, 2H), 0.99–0.94 (m, 2H).

2-(Cyclopropanecarboxamido)-N-(4-(cyclopropylmethoxy)-pyridin-3-yl)isonicotinamide (24). MS (ESI) (*m/z*): 353 (*M* + *H*)⁺; ¹H NMR (400 MHz, DMSO-*d*₆) δ 11.03 (s, 1H), 9.98 (s, 1H), 8.57 (s, 2H), 8.51 (d, *J* = 5.1 Hz, 1H), 8.34 (d, *J* = 5.7 Hz, 1H), 7.56 (d, *J* = 5.0 Hz, 1H), 7.16 (d, *J* = 5.7 Hz, 1H), 4.01 (d, *J* = 6.8 Hz, 2H), 2.10–1.98 (m, 1H), 1.27–1.23 (m, 1H), 0.86 (d, *J* = 6.1 Hz, 4H), 0.59–0.51 (m, 2H), 0.42–0.32 (m, 2H).

2-(Cyclopropanecarboxamido)-N-(4-(2-hydroxyethoxy)pyridin-3-yl)isonicotinamide (25). MS (ESI) (*m/z*): 343 (*M* + *H*)⁺; ¹H NMR (500 MHz, DMSO-*d*₆) δ 11.04 (s, 1H), 8.75 (s, 1H), 8.54 (s, 1H), 8.51 (d, *J* = 5.0 Hz, 1H), 8.32 (d, *J* = 5.6 Hz, 1H), 7.55 (d, *J* = 4.4 Hz, 1H), 7.19 (d, *J* = 5.7 Hz, 1H), 4.16 (t, *J* = 4.8 Hz, 2H), 3.78–3.71 (m, 2H), 2.06 (s, 1H), 0.91–0.85 (m, 4H).

Methyl 2-(N-(Cyclopropanecarbonyl)-cyclopropanecarboxamido)isonicotinate (9). Cyclopropanecarbonyl chloride (3.79 mL, 41.4 mmol) was added to a solution of methyl 2-aminoisonicotinamide (3.0 g, 19.72 mmol) and Hünig's base (7.23 mL, 41.4 mmol) in methylene chloride (150 mL) at 0 °C. The reaction was stirred at 0 °C for 1 h before quenching with water. The mixture was diluted with methylene chloride and washed with NaHCO₃ (sat.) and water. The organic layer was separated, dried (Na₂SO₄), filtered, and concentrated. Flash column chromatography, eluting with ethyl acetate in hexane (0–50%), afforded the desired product (4.99 g, 88%) as a white solid: MS (ESI) (*m/z*): 311 (*M* + Na)⁺.

2-(Cyclopropanecarboxamido)isonicotinic Acid (10). A mixture of LiOH (8.65 mL, 69.2 mmol, 8 M in water) and 9 (4.99 g, 17.31 mmol) in tetrahydrofuran (20 mL) and methanol (2 mL) was stirred at room temperature for 18 h. The volatile components were removed

in vacuo, and the residue was acidified by adding 1 N HCl. The solid was filtered and washed with water. The white solid was used without further purification after drying under high vacuum for several hours (2.81 g, 79%): ¹H NMR (400 MHz, DMSO-*d*₆) δ 11.02 (s, 1H), 8.56 (s, 1H), 8.48 (dd, *J* = 5.3, 0.8 Hz, 1H), 7.51 (dd, *J* = 5.0, 1.5 Hz, 1H), 2.06–1.98 (m, 1H), 0.88–0.81 (m, 4H).

2-(Cyclopropanecarboxamido)-N-(4-phenoxy)pyridin-3-yl)-isonicotinamide (22). To a 5 mL round-bottomed flask was added 10 (34 mg, 0.165 mmol) in CH₂Cl₂ (1 mL) to give a white suspension. DMF (2.55 μL, 0.033 mmol) (one drop) and oxalyl chloride (0.017 mL, 0.198 mmol) were added. The mixture was stirred at rt for 30 min. 4-Phenoxypyridin-3-amine (30.7 mg, 0.165 mmol) and Et₃N (0.069 mL, 0.495 mmol) were added. The mixture was stirred at rt overnight. The reaction mixture was concentrated, redissolved in 1.5 mL of MeOH, and purified by prep-HPLC to afford the desired product (21.3 mg, 35%): MS (ESI) (*m/z*): 375 (*M* + *H*)⁺; ¹H NMR (500 MHz, DMSO-*d*₆) δ 11.02 (s, 1H), 10.41 (s, 1H), 8.71 (s, 1H), 8.55 (s, 1H), 8.52–8.43 (m, 1H), 8.34 (d, *J* = 5.6 Hz, 1H), 7.54–7.50 (m, 1H), 7.50–7.45 (m, 2H), 7.31–7.25 (m, 1H), 7.20–7.15 (m, 2H), 6.79 (d, *J* = 5.6 Hz, 1H), 2.09–1.99 (m, 1H), 0.88–0.79 (m, 4H).

2-(Cyclopropanecarboxamido)-N-(4-(trifluoromethyl)pyridin-3-yl)isonicotinamide (17). MS (ESI) (*m/z*): 351 (*M* + *H*)⁺; ¹H NMR (500 MHz, DMSO-*d*₆) δ 11.04 (s, 1H), 10.80–10.64 (s, br, 1H), 8.85 (s, 1H), 8.78 (d, *J* = 4.9 Hz, 1H), 8.59 (s, 1H), 8.53 (d, *J* = 5.2 Hz, 1H), 7.85 (d, *J* = 4.9 Hz, 1H), 7.56 (dd, *J* = 5.0, 1.4 Hz, 1H), 2.12–2.01 (m, 1H), 0.92–0.82 (m, 4H).

2-(Cyclopropanecarboxamido)-N-(4-(neopentyloxy)pyridin-3-yl)-isonicotinamide (23). To a 5 mL vial were added 4-(neopentyloxy)-pyridin-3-amine (24 mg, 0.133 mmol) and 10 (27.5 mg, 0.133 mmol) in DMF (1 mL) to give a tan solution. HATU (101 mg, 0.266 mmol) and Hunig's base (0.047 mL, 0.266 mmol) were added, and the mixture was stirred at rt for 18 h. The reaction mixture was purified by prep-HPLC to afford the desired product (32 mg, 65%): MS (ESI) (*m/z*): 369 (*M* + *H*)⁺; ¹H NMR (400 MHz, DMSO-*d*₆) δ 10.98 (s, 1H), 9.97 (s, 1H), 8.56 (s, 1H), 8.51 (dd, *J* = 5.1, 0.6 Hz, 1H), 8.49 (s, 1H), 8.36 (d, *J* = 5.6 Hz, 1H), 7.53 (dd, *J* = 5.1, 1.4 Hz, 1H), 7.16 (d, *J* = 5.7 Hz, 1H), 3.77 (s, 2H), 2.12–1.99 (m, 1H), 0.96 (s, 9H), 0.90–0.83 (m, 4H).

2-(Cyclopropanecarboxamido)-N-(2-fluoropyridin-3-yl)-isonicotinamide (12). MS (ESI) (*m/z*): 301 (*M* + *H*)⁺; ¹H NMR (500 MHz, DMSO-*d*₆) δ 11.06 (s, 1H), 10.61 (s, 1H), 8.57 (d, *J* = 0.5 Hz, 1H), 8.53 (dd, *J* = 5.1, 0.6 Hz, 1H), 8.20 (ddd, *J* = 9.6, 7.8, 1.7 Hz, 1H), 8.15–8.09 (m, 1H), 7.56 (dd, *J* = 5.1, 1.6 Hz, 1H), 7.48–7.40 (m, 1H), 2.11–2.00 (m, 1H), 0.92–0.81 (m, 4H).

2-(Cyclopropanecarboxamido)-N-(2-hydroxypyridin-3-yl)-isonicotinamide (13). MS (ESI) (*m/z*): 299 (*M* + *H*)⁺; ¹H NMR (500 MHz, DMSO-*d*₆) δ 12.18 (s, 1H), 11.08 (s, 1H), 9.44 (s, 1H), 8.61–8.44 (m, 2H), 8.30 (dd, *J* = 7.3, 1.8 Hz, 1H), 7.51 (dd, *J* = 5.1, 1.6 Hz, 1H), 7.23 (dd, *J* = 6.6, 1.8 Hz, 1H), 6.42–6.22 (m, 1H), 2.05 (dq, *J* = 7.5, 5.0 Hz, 1H), 0.93–0.81 (m, 4H).

2-(Cyclopropanecarboxamido)-N-(2-cyanopyridin-3-yl)-isonicotinamide (14). MS (ESI) (*m/z*): 308 (*M* + *H*)⁺; ¹H NMR (500 MHz, DMSO-*d*₆) δ 11.01 (s, 1H), 8.62 (s, 1H), 8.51 (d, *J* = 4.9 Hz, 2H), 8.21 (dd, *J* = 8.4, 1.3 Hz, 1H), 7.73 (dd, *J* = 8.4, 4.6 Hz, 1H), 7.64 (dd, *J* = 5.1, 1.5 Hz, 1H), 2.09–1.99 (m, 1H), 0.91–0.81 (m, 4H).

2-(Cyclopropanecarboxamido)-N-(4-iodopyridin-3-yl)-isonicotinamide (26). To a 250 mL round-bottomed flask was added 10 (776.5 mg, 3.77 mmol) in CH₂Cl₂ (30 mL) to give a white suspension. After cooling to 0 °C, DMF (0.029 mL, 0.377 mmol) and oxalyl chloride (0.363 mL, 4.14 mmol) were added. The mixture was stirred at 0 °C for 2 h. LCMS showed the desired chloride (as methyl ester form). 4-Iodopyridin-3-amine (829 mg, 3.77 mmol) was added at 0 °C, followed by Et₃N (2.1 mL, 15.06 mmol). The mixture became clear to a tan solution. It was concentrated to a tan oil. The residue was purified by FCC up to 10% MeOH/CH₂Cl₂ (contains 1% AcOH). The product peak was pooled and concentrated to a tan solid (100%), which was used without further characterization.

N-(4-Chloropyridin-3-yl)-2-(cyclopropanecarboxamido)-isonicotinamide (16). MS (ESI) (*m/z*): 317 (*M* + *H*)⁺; ¹H NMR (400 MHz, CDCl₃) δ 9.60 (s, 1H), 8.76 (s, 1H), 8.71 (d, *J* = 0.7 Hz,

1H), 8.49 (dd, $J = 5.1, 0.7$ Hz, 1H), 8.42 (s, 1H), 8.38 (d, $J = 5.3$ Hz, 1H), 7.59 (dd, $J = 5.1, 1.6$ Hz, 1H), 7.42 (d, $J = 5.2$ Hz, 1H), 1.69–1.58 (m, 1H), 1.20–1.13 (m, 2H), 1.00–0.93 (m, 2H).

2-(Cyclopropanecarboxamido)-N-(4-(2-fluorophenyl)pyridin-3-yl)isonicotinamide (27). To a 5 mL microwave tube were added **26** (36.6 mg, 0.090 mmol), (2-fluorophenyl)boronic acid (20.07 mg, 0.143 mmol), and Na_2CO_3 (0.134 mL, 0.269 mmol) in dioxane (0.8 mL) to give a tan suspension under nitrogen. 1,1'-Bis-(diphenylphosphino)ferrocenepalladium(II) dichloride, toluene (3.69 mg, 4.48 μmol) was added under nitrogen. The vial was sealed and heated at 140 °C for 45 min. It was filtered and purified by prep-HPLC to afford the desired product (7.2 mg, 21%): ^1H NMR (500 MHz, $\text{DMSO}-d_6$) δ 10.98 (s, 1H), 10.41 (s, 1H), 8.70 (s, 1H), 8.58 (d, $J = 5.0$ Hz, 1H), 8.43 (d, $J = 5.2$ Hz, 1H), 8.40 (s, 1H), 7.49 (d, $J = 5.0$ Hz, 1H), 7.47–7.38 (m, 2H), 7.35–7.22 (m, 3H), 2.03 (dq, $J = 7.1, 5.4$ Hz, 1H), 0.89–0.81 (m, 4H).

2-(Cyclopropanecarboxamido)-N-(4-(3-fluorophenyl)pyridin-3-yl)isonicotinamide (28). MS (ESI) (m/z): 377 ($\text{M} + \text{H}^+$); ^1H NMR (500 MHz, $\text{DMSO}-d_6$) δ 11.00 (s, 1H), 10.47 (s, 1H), 8.66 (s, 1H), 8.59 (d, $J = 5.0$ Hz, 1H), 8.49–8.43 (m, 2H), 7.52 (d, $J = 5.0$ Hz, 1H), 7.51–7.44 (m, 1H), 7.40 (d, $J = 4.9$ Hz, 1H), 7.35 (d, $J = 8.0$ Hz, 2H), 7.27–7.21 (m, 1H), 2.08–1.99 (m, 1H), 0.89–0.81 (m, 4H).

2-(Cyclopropanecarboxamido)-N-(4-(4-fluorophenyl)pyridin-3-yl)isonicotinamide (29). HRMS (ESI) (m/z): calcd for $\text{C}_{21}\text{H}_{18}\text{O}_2\text{N}_4\text{F}$, 377.1408 ($\text{M} + \text{H}^+$); found, 377.1398; ^1H NMR (500 MHz, $\text{DMSO}-d_6$) δ 11.00 (s, 1H), 10.42 (s, 1H), 8.65 (s, 1H), 8.57 (d, $J = 5.0$ Hz, 1H), 8.50–8.41 (m, 2H), 7.56 (dd, $J = 8.7, 5.5$ Hz, 2H), 7.49 (d, $J = 5.0$ Hz, 1H), 7.40 (d, $J = 4.7$ Hz, 1H), 7.35–7.24 (m, 2H), 2.10–1.98 (m, 1H), 0.88–0.82 (m, 4H).

2-(Cyclopropanecarboxamido)-N-(4-(4-methoxyphenyl)pyridin-3-yl)isonicotinamide (30). MS (ESI) (m/z): 389 ($\text{M} + \text{H}^+$); ^1H NMR (500 MHz, $\text{DMSO}-d_6$) δ 11.01 (s, 1H), 10.38 (s, 1H), 8.60 (s, 1H), 8.54 (d, $J = 5.0$ Hz, 1H), 8.47 (d, $J = 5.0$ Hz, 2H), 7.47 (dd, $J = 9.8, 6.9$ Hz, 3H), 7.43 (d, $J = 6.2$ Hz, 1H), 7.05–7.01 (m, 2H), 3.79 (s, 3H), 2.10–1.96 (m, 1H), 0.91–0.79 (m, 4H).

2-(Cyclopropanecarboxamido)-N-(4-(4-(trifluoromethoxy)phenyl)pyridin-3-yl)isonicotinamide (31). MS (ESI) (m/z): 443 ($\text{M} + \text{H}^+$); ^1H NMR (500 MHz, $\text{DMSO}-d_6$) δ 11.01 (s, 1H), 10.46 (s, 1H), 8.71 (s, 1H), 8.61 (d, $J = 5.1$ Hz, 1H), 8.46 (d, $J = 5.2$ Hz, 1H), 8.44 (s, 1H), 7.66 (s, 1H), 7.64 (s, 1H), 7.55 (d, $J = 5.0$ Hz, 1H), 7.48 (s, 1H), 7.46 (s, 1H), 7.38 (d, $J = 5.0$ Hz, 1H), 2.10–1.98 (m, 1H), 0.92–0.79 (m, 4H).

N-(4-(4-Cyanophenyl)pyridin-3-yl)-2-(cyclopropanecarboxamido)isonicotinamide (32). MS (ESI) (m/z): 384 ($\text{M} + \text{H}^+$); ^1H NMR (500 MHz, $\text{DMSO}-d_6$) δ 11.01 (s, 1H), 10.50 (s, 1H), 8.72 (s, 1H), 8.61 (d, $J = 5.0$ Hz, 1H), 8.46 (d, $J = 5.1$ Hz, 1H), 8.40 (s, 1H), 7.95–7.90 (m, 2H), 7.70 (d, $J = 8.4$ Hz, 2H), 7.53 (d, $J = 5.1$ Hz, 1H), 7.39 (d, $J = 4.0$ Hz, 1H), 2.09–1.99 (m, 1H), 0.86 (dtd, $J = 8.0, 5.0, 3.1$ Hz, 4H).

N-(4-(4-Chlorophenyl)pyridin-3-yl)-2-(cyclopropanecarboxamido)isonicotinamide (33). HRMS (ESI) (m/z): calcd for $\text{C}_{21}\text{H}_{18}\text{O}_2\text{N}_4\text{Cl}$, 393.1113 ($\text{M} + \text{H}^+$); found, 393.1104; ^1H NMR (500 MHz, $\text{DMSO}-d_6$) δ 11.01 (s, 1H), 10.44 (s, 1H), 8.67 (s, 1H), 8.58 (d, $J = 5.0$ Hz, 1H), 8.52–8.40 (m, 2H), 7.56–7.51 (m, 4H), 7.50 (d, $J = 5.1$ Hz, 1H), 7.41 (d, $J = 4.0$ Hz, 1H), 2.04 (dq, $J = 7.5, 5.0$ Hz, 1H), 0.92–0.80 (m, 4H).

2-(Cyclopropanecarboxamido)-N-(4-(4-(difluoromethoxy)phenyl)pyridin-3-yl)isonicotinamide (34). MS (ESI) (m/z): 425 ($\text{M} + \text{H}^+$); ^1H NMR (500 MHz, $\text{DMSO}-d_6$) δ 11.00 (s, 1H), 10.42 (s, 1H), 8.66 (s, 1H), 8.57 (d, $J = 4.9$ Hz, 1H), 8.46 (d, $J = 5.2$ Hz, 1H), 8.43 (s, 1H), 7.59 (d, $J = 8.5$ Hz, 2H), 7.49 (d, $J = 4.9$ Hz, 1H), 7.41 (d, $J = 5.2$ Hz, 1H), 7.31–7.25 (m, 3H), 2.08–1.99 (m, 1H), 0.88–0.82 (m, 4H).

2-(Cyclopropanecarboxamido)-N-(4-(4-(methyl)phenyl)pyridin-3-yl)isonicotinamide (35). MS (ESI) (m/z): 373 ($\text{M} + \text{H}^+$); ^1H NMR (500 MHz, $\text{DMSO}-d_6$) δ 11.00 (s, 1H), 10.38 (s, 1H), 8.62 (s, 1H), 8.56 (d, $J = 5.0$ Hz, 1H), 8.51–8.42 (m, 2H), 7.47 (d, $J = 5.0$ Hz, 1H), 7.42 (d, $J = 7.8$ Hz, 3H), 7.27 (d, $J = 7.9$ Hz, 2H), 2.32 (s, 3H), 2.10–1.99 (m, 1H), 0.90–0.80 (m, 4H).

N-(4-(4-(tert-Butyl)phenyl)pyridin-3-yl)-2-(cyclopropanecarboxamido)isonicotinamide (36). MS (ESI) (m/z):

415 ($\text{M} + \text{H}^+$); ^1H NMR (500 MHz, $\text{DMSO}-d_6$) δ 11.00 (s, 1H), 10.38 (s, 1H), 8.65 (s, 1H), 8.55 (d, $J = 5.2$ Hz, 1H), 8.49–8.43 (m, 2H), 7.54–7.46 (m, 5H), 7.41 (d, $J = 4.6$ Hz, 1H), 2.08–1.99 (m, 1H), 1.30 (s, 9H), 0.87–0.82 (m, 4H).

2-(Cyclopropanecarboxamido)-N-(4-(2-(trifluoromethyl)phenyl)pyridin-3-yl)isonicotinamide (37). MS (ESI) (m/z): 427 ($\text{M} + \text{H}^+$); ^1H NMR (500 MHz, $\text{DMSO}-d_6$) δ 10.95 (s, 1H), 10.19 (s, 1H), 8.72 (s, 1H), 8.56 (d, $J = 4.9$ Hz, 1H), 8.39 (d, $J = 5.2$ Hz, 1H), 8.31 (s, 1H), 7.83 (d, $J = 7.6$ Hz, 1H), 7.73–7.67 (m, 1H), 7.65–7.59 (m, 1H), 7.40 (d, $J = 7.6$ Hz, 1H), 7.36 (d, $J = 5.2$ Hz, 1H), 7.20 (dd, $J = 5.0, 1.4$ Hz, 1H), 2.05–1.98 (m, 1H), 0.86–0.81 (m, 4H).

2-(Cyclopropanecarboxamido)-N-(4-(2-chlorophenyl)pyridin-3-yl)isonicotinamide (38). MS (ESI) (m/z): 393 ($\text{M} + \text{H}^+$); ^1H NMR (500 MHz, $\text{DMSO}-d_6$) δ 11.02 (s, 1H), 10.58 (s, 1H), 8.94 (s, 1H), 8.72 (d, $J = 5.2$ Hz, 1H), 8.44 (d, $J = 5.2$ Hz, 1H), 8.37 (s, 1H), 7.71 (d, $J = 5.5$ Hz, 1H), 7.60–7.56 (m, 1H), 7.48–7.40 (m, 3H), 7.30 (dd, $J = 5.2, 1.2$ Hz, 1H), 2.03 (quin, $J = 6.2$ Hz, 1H), 0.86–0.83 (m, 4H).

2-(Cyclopropanecarboxamido)-N-(4-(2,4-difluorophenyl)pyridin-3-yl)isonicotinamide (39). MS (ESI) (m/z): 395 ($\text{M} + \text{H}^+$); ^1H NMR (500 MHz, $\text{DMSO}-d_6$) δ 10.99 (s, 1H), 10.40 (br. s., 1H), 8.73 (s, 1H), 8.58 (d, $J = 4.9$ Hz, 1H), 8.45 (d, $J = 4.9$ Hz, 1H), 8.39 (s, 1H), 7.51–7.43 (m, 2H), 7.39–7.29 (m, 2H), 7.18 (td, $J = 8.5, 2.4$ Hz, 1H), 2.09–2.00 (m, 1H), 0.89–0.80 (m, 4H).

2-(Cyclopropanecarboxamido)-N-(4-(2,4-dichlorophenyl)pyridin-3-yl)isonicotinamide (40). MS (ESI) (m/z): 427 ($\text{M} + \text{H}^+$); ^1H NMR (500 MHz, $\text{DMSO}-d_6$) δ 10.98 (s, 1H), 10.34 (br. s., 1H), 8.77 (s, 1H), 8.58 (d, $J = 5.2$ Hz, 1H), 8.44 (d, $J = 4.9$ Hz, 1H), 8.35 (s, 1H), 7.73 (d, $J = 1.8$ Hz, 1H), 7.51 (dd, $J = 8.2, 2.1$ Hz, 1H), 7.43 (d, $J = 5.2$ Hz, 1H), 7.39 (d, $J = 8.2$ Hz, 1H), 7.31 (d, $J = 4.0$ Hz, 1H), 2.06–1.99 (m, 1H), 0.89–0.82 (m, 4H).

N-(4-(2-Chloro-4-fluorophenyl)pyridin-3-yl)-2-(cyclopropanecarboxamido)isonicotinamide (41). MS (ESI) (m/z): 393 ($\text{M} + \text{H}^+$); ^1H NMR (500 MHz, $\text{DMSO}-d_6$) δ 10.98 (s, 1H), 10.32 (br. s., 1H), 8.75 (s, 1H), 8.57 (d, $J = 4.9$ Hz, 1H), 8.43 (d, $J = 5.2$ Hz, 1H), 8.35 (s, 1H), 7.55 (dd, $J = 9.0, 2.6$ Hz, 1H), 7.45–7.39 (m, 2H), 7.34–7.27 (m, 2H), 2.05–1.99 (m, 1H), 0.87–0.83 (m, 4H).

2-(Cyclopropanecarboxamido)-N-(4-(4-fluoro-2-(trifluoromethyl)phenyl)pyridin-3-yl)isonicotinamide (42). MS (ESI) (m/z): 445 ($\text{M} + \text{H}^+$); ^1H NMR (500 MHz, $\text{DMSO}-d_6$) δ 10.96 (s, 1H), 10.17 (br. s., 1H), 8.77 (s, 1H), 8.55 (d, $J = 5.2$ Hz, 1H), 8.41 (d, $J = 4.9$ Hz, 1H), 8.28 (s, 1H), 7.75 (dd, $J = 9.3, 2.6$ Hz, 1H), 7.60 (td, $J = 8.5, 2.6$ Hz, 1H), 7.46 (dd, $J = 8.7, 5.6$ Hz, 1H), 7.36 (d, $J = 4.9$ Hz, 1H), 7.23 (dd, $J = 5.2, 1.2$ Hz, 1H), 2.06–1.96 (m, 1H), 0.87–0.81 (m, 4H).

N-(4-(4-Chloro-2-fluorophenyl)pyridin-3-yl)-2-(cyclopropanecarboxamido)isonicotinamide (43). MS (ESI) (m/z): 411 ($\text{M} + \text{H}^+$); ^1H NMR (500 MHz, $\text{DMSO}-d_6$) δ 11.00 (s, 1H), 10.42 (br. s., 1H), 8.75 (s, 1H), 8.57 (d, $J = 4.9$ Hz, 1H), 8.45 (d, $J = 5.2$ Hz, 1H), 8.39 (s, 1H), 7.55 (dd, $J = 10.1, 2.1$ Hz, 1H), 7.50–7.43 (m, 2H), 7.41–7.32 (m, 2H), 2.08–1.99 (m, 1H), 0.90–0.82 (m, 4H).

2-(Cyclopropanecarboxamido)-N-(4-(2,5-difluorophenyl)pyridin-3-yl)isonicotinamide (44). MS (ESI) (m/z): 395 ($\text{M} + \text{H}^+$); ^1H NMR (500 MHz, $\text{DMSO}-d_6$) δ 10.99 (s, 1H), 10.46 (br. s., 1H), 8.72 (s, 1H), 8.60 (d, $J = 4.9$ Hz, 1H), 8.45 (d, $J = 5.2$ Hz, 1H), 8.40 (s, 1H), 7.51 (d, $J = 5.2$ Hz, 1H), 7.40–7.25 (m, 4H), 2.07–1.98 (m, 1H), 0.87–0.82 (m, 4H).

2-(Cyclopropanecarboxamido)-N-(4-(2,3-difluorophenyl)pyridin-3-yl)isonicotinamide (45). MS (ESI) (m/z): 395 ($\text{M} + \text{H}^+$); ^1H NMR (500 MHz, $\text{DMSO}-d_6$) δ 10.97 (s, 1H), 8.75 (s, 1H), 8.57 (d, $J = 4.9$ Hz, 1H), 8.43 (d, $J = 5.2$ Hz, 1H), 8.39 (s, 1H), 7.51 (d, $J = 4.9$ Hz, 1H), 7.46 (q, $J = 8.5$ Hz, 1H), 7.34 (d, $J = 4.6$ Hz, 1H), 7.30–7.19 (m, 2H), 2.07–1.99 (m, 1H), 0.87–0.81 (m, 4H).

GSK-3 β /3 α Kinase Assay. Inhibitors were evaluated in a competitive binding assay for their ability to bind to GSK-3 α and GSK-3 β . Test compound was incubated in assay buffer (20 mM Hepes, pH 7.4, 10 mM MgCl_2 , 0.015% Brij-35, 4 mM DTT, 0.05 mg/mL BSA) in the presence of 1 nM GST-GSK-3 α or GST-GSK-3 β , a fluorescently labeled small molecule at K_d (GSK-3 α = 15 nM; GSK-3 β = 6 nM), and 0.2 nM anti-GST labeled detection antibody. After a 1 h incubation at room temperature, homogeneous time-resolved fluorescence (HTRF) was monitored on a Envision plate reader (Ex

340 nm; Em 520/615 nm). Inhibition data were calculated by comparison of the no enzyme control reactions for 100% inhibition and vehicle-only reactions for 0% inhibition. Dose–response curves were generated to determine the concentration required to inhibit 50% of the kinase activity (IC_{50}).

Triple-Transgenic Mouse Model.⁴⁹ Mice were handled strictly according to Bristol-Myers Squibb (BMS) Animal Care and Use Committee guidelines. 3XTg mice were obtained from Dr. Frank LaFerla at the University of California, Irvine. The mice were bred onto the C57BL/6 background by Dr. Mark Mattson (National Institute on Aging), and breeders from those congenic mice were obtained by BMS, where they were bred as homozygotes. Mice were housed with a 6 am–6 pm light/dark cycle and allowed free access to food and water. Animals were used for study between the ages of 5 to 7 months. Test compounds were dosed at 30 mg/kg as a nanosuspension in 2% HPC-SSL/0.15% SLS/97.85% water by oral gavage. LiCl was administered at 250 mg/kg by ip injection in water. Animals were euthanized by guillotine 5 h postdose. Brains were dissected into hemispheres, flash frozen in liquid nitrogen, and stored at -80°C until processing. Each hemisphere was homogenized in T-PER tissue protein extraction buffer (Thermo Scientific, Rockford, IL) supplemented with phosphatase inhibitor cocktail sets I and II (Sigma-Aldrich, St. Louis, MO), complete protease inhibitor EDTA-free (Roche, Indianapolis, IN), 7 μM pepstatin (Sigma-Aldrich, St. Louis, MO), and 1 mM PMSF (Sigma, St. Louis, MO) using a Potter-Elvehjem homogenizer. Homogenate was centrifuged at 100 000g for 30 min at 4°C . Cleared homogenate was frozen and stored at -80°C . Commercial total tau human (KHB0041) and tau[S396] human (KHB7031) ELISA kits (Invitrogen, Grand Island, NY) were used as directed to determine total and S396 phosphorylated human tau levels in the cleared homogenates, respectively. Each sample was tested in triplicate, and compound-treated animal groups were compared to vehicle-treated animal groups with statistical analysis using Student's *t* test.

■ ASSOCIATED CONTENT

Supporting Information

The Supporting Information is available free of charge on the ACS Publications website at DOI: 10.1021/acs.jmedchem.5b01550.

SMILES strings and GSK-3 β / α and pTau IC_{50} data for 11–45 (CSV)

Synthesis and characterization of the aminopyridine intermediates from Scheme 2; X-ray crystal studies of 15 and 18 bound to GSK-3 β ; biological assays; and related Ambit graphs (PDF)

■ AUTHOR INFORMATION

Corresponding Author

*E-mail: guanglin.luo@bms.com. Phone: 203-677-6640. Fax: 203-677-7702.

Notes

The authors declare no competing financial interest.

■ ACKNOWLEDGMENTS

We thank Spectrix chemists for all of the final compound purification and characterizations.

■ ABBREVIATIONS USED

GSK-3, glycogen synthase kinase-3; AD, Alzheimer's disease; A β , beta-amyloid; NFTs, neurofibrillary tangles; PKB (AKT), protein kinase B; PHFs, paired helical filaments; b/p ratio, brain/plasma ratio; pTau, phosphorylated Tau; Pgp, P-glycoprotein; HPLC, high-pressure liquid chromatography; LCMS, liquid chromatography–mass spectrometry; FCC,

flash column chromatography; NMR, nuclear magnetic resonance; SAR, structure–activity relationship; po, taken orally; ip, intraperitoneal

■ REFERENCES

- (1) Alzheimer's Association. Alzheimer's Disease Facts and Figures. *Alzheimer's Dementia* **2013**, 9, 208–245.
- (2) Hardy, J. Alzheimer's disease: the amyloid cascade hypothesis: an update and reappraisal. *J. Alzheimer's Dis.* **2006**, 9, 151–153.
- (3) Zaghi, J.; Goldenson, B.; Inayathullah, M.; Lossinsky, A. S.; Masoumi, A.; Avagyan, H.; Mahanian, M.; Bernas, M.; Weinand, M.; Rosenthal, M. J.; Espinosa-Jeffrey, A.; de Vellis, J.; Teplow, D. B.; Fiala, M. Alzheimer disease macrophages shuttle amyloid-beta from neurons to vessels, contributing to amyloid angiopathy. *Acta Neuropathol.* **2009**, 117, 111–124.
- (4) Grimes, C. A.; Jope, R. S. The multifaceted roles of glycogen synthase kinase 3 β in cellular signaling. *Prog. Neurobiol.* **2001**, 65, 391–426.
- (5) Woodgett, J. R. Molecular cloning and expression of glycogen synthase kinase-3/factor A. *EMBO J.* **1990**, 9, 2431–2438.
- (6) Pei, J. J.; Tanaka, T.; Tung, Y. C.; Braak, E.; Iqbal, K.; Grundke-Iqbal, I. Distribution, levels, and activity of glycogen synthase kinase-3 in the Alzheimer disease brain. *J. Neuropathol. Exp. Neurol.* **1997**, 56, 70–78.
- (7) Pei, J. J.; Braak, E.; Braak, H.; Grundke-Iqbal, I.; Iqbal, K.; Winblad, B.; Cowburn, R. F. Distribution of active glycogen synthase kinase 3 β (GSK-3 β) in brains staged for Alzheimer disease neurofibrillary changes. *J. Neuropathol. Exp. Neurol.* **1999**, 58, 1010–1019.
- (8) Leroy, K.; Brion, J.-P. Developmental expression and localization of glycogen synthase kinase-3 β in rat brain. *J. Chem. Neuroanat.* **1999**, 16, 279–293.
- (9) Sereno, L.; Coma, M.; Rodriguez, M.; Sanchez-Ferrer, P.; Sanchez, M. B.; Gich, I.; Agullo, J. M.; Perez, M.; Avila, J.; Guardia-Laguarta, C.; Clarimon, J.; Lleo, A.; Gómez-Isla, T. A novel GSK-3 β inhibitor reduces Alzheimer's pathology and rescues neuronal loss in vivo. *Neurobiol. Dis.* **2009**, 35, 359–367.
- (10) Takashima, A. Drug development targeting the glycogen synthase kinase-3 β (GSK-3 β)-mediated signal transduction pathway: role of GSK-3 β in adult brain. *J. Pharmacol. Sci.* **2009**, 109, 174–178.
- (11) Doble, B. W.; Patel, S.; Wood, G. A.; Kockeritz, L. K.; Woodgett, J. R. Functional redundancy of GSK-3 α and GSK-3 β in Wnt/ β -catenin signaling shown by using an allelic series of embryonic stem cell lines. *Dev. Cell* **2007**, 12, 957–971.
- (12) Sutherland, C. What Are the bona fide GSK3 Substrates? *Int. J. Alzheimer's Dis.* **2011**, 2011, 505607.
- (13) Cross, D. A.; Alessi, D. R.; Cohen, P.; Andjelkovich, M.; Hemmings, B. A. Inhibition of glycogen synthase kinase-3 by insulin mediated by protein kinase B. *Nature* **1995**, 378, 785–789.
- (14) Hanger, D. P.; Noble, W. Functional implications of glycogen synthase kinase-3-mediated Tau phosphorylation. *Int. J. Alzheimer's Dis.* **2011**, 2011, 1–11.
- (15) Stebbings, H. Microtubule-based intracellular transport of organelles. *Cytoskeleton* **1995**, 2, 113–140.
- (16) Grundke-Iqbal, I.; Iqbal, K.; Quinlan, M.; Tung, Y. C.; Zaidi, M. S.; Wisniewski, H. M. Microtubule-associated protein tau. A component of Alzheimer paired helical filaments. *J. Biol. Chem.* **1986**, 261, 6084–6089.
- (17) Grundke-Iqbal, I.; Iqbal, K.; Tung, Y. C.; Quinlan, M.; Wisniewski, H. M.; Binder, L. I. Abnormal phosphorylation of the microtubule-associated protein tau (tau) in Alzheimer cytoskeletal pathology. *Proc. Natl. Acad. Sci. U. S. A.* **1986**, 83, 4913–4917.
- (18) Iqbal, K.; Grundke-Iqbal, I. Discoveries of tau, abnormally hyperphosphorylated tau and others of neurofibrillary degeneration: a personal historical perspective. *J. Alzheimer's Dis.* **2006**, 9, 219–242.
- (19) Maixner, D. W.; Weng, H.-R. The Role of Glycogen Synthase Kinase 3 Beta in Neuroinflammation and Pain. *J. Pharm. Pharmacol.* **2013**, 1, 001.

- (20) Gomez-Sintes, R.; Hernandez, F.; Lucas, J. J.; Avila, J. GSK-3 Mouse Models to Study Neuronal Apoptosis and Neurodegeneration. *Front. Mol. Neurosci.* **2011**, *4*, 45.
- (21) Takashima, A. GSK-3 β and memory formation. *Front. Mol. Neurosci.* **2012**, *5*, 47.
- (22) (a) Domínguez, J. M.; Fuertes, A.; Orozco, L.; del Monte-Millán, M.; Delgado, E.; Medina, M. Evidence for Irreversible Inhibition of Glycogen Synthase Kinase-3 by Tideglusib. *J. Biol. Chem.* **2012**, *287* (2), 893–904. (b) Del Ser, T.; Steinwachs, K. C.; Gertz, H. J.; Andrés, M. V.; Gómez-Carrillo, B.; Medina, M.; Vericat, J. A.; Redondo, P.; Fleet, D.; Leon, T. Treatment of Alzheimer's disease with the GSK-3 inhibitor tideglusib: A pilot study. *J. Alzheimer's Dis.* **2013**, *33*, 205–215.
- (23) Rowe, M. K.; Wiest, C.; Chuang, D.-M. GSK-3 is a viable potential target for therapeutic intervention in bipolar disorder. *Neurosci. Biobehav. Rev.* **2007**, *31*, 920–931.
- (24) Henriksen, E. J.; Kinnick, T. R.; Teachey, M. K.; O'Keefe, M. P.; Ring, D.; Johnson, K. W.; Harrison, S. D. Modulation of Muscle Insulin Resistance by Selective Inhibition of Glycogen Synthase Kinase-3 in Zucker Diabetic Fatty Rats. *Am. J. Physiol. Endocrinol. Metab.* **2003**, *284* (5), E892–900.
- (25) Marsell, R.; Sisask, G.; Nilsson, Y.; Sundgren-Andersson, A. K.; Andersson, U.; Larsson, S.; Nilsson, O.; Ljunggren, O.; Jonsson, K. B. GSK-3 inhibition by an orally active small molecule increases bone mass in rats. *Bone* **2012**, *50* (3), 619–627.
- (26) Doble, B.; Woodgett, J. R. GSK-3: tricks of the trade for a multitasking kinase. *J. Cell Sci.* **2003**, *116*, 1175–1186.
- (27) (a) Kitano, A.; Shimasaki, T.; Chikano, Y.; Nakada, M.; Hirose, M.; Higashi, T.; Ishigaki, Y.; Endo, Y.; Takino, T.; Sato, H.; Sai, Y.; Miyamoto, K.; Motoo, Y.; Kawakami, K.; Minamoto, T. Aberrant glycogen synthase kinase 3 β is involved in pancreatic cancer cell invasion and resistance to therapy. *PLoS One* **2013**, *8* (2), e55289. (b) McCubrey, J. A.; Steelman, L. S.; Bertrand, F. E.; Davis, N. M.; Sokolosky, M.; Abrams, S. L.; Montalto, G.; D'Assoro, A. B.; Libra, M.; Nicoletti, F.; Maestro, R.; Basecke, J.; Rakus, D.; Gizak, A.; Demidenko, Z.; Cocco, L.; Martelli, A. M.; Cervello, M. GSK-3 as potential target for therapeutic intervention in cancer. *Oncotarget* **2014**, *5* (10), 2881–2911.
- (28) Gray, J. E.; Infante, J. R.; Brail, L. H.; Simon, G. R.; Cooksey, J. F.; Jones, S. F.; Farrington, D. L.; Yeo, A.; Jackson, K. A.; Chow, K. H.; Zamek-Gliszczynski, M. J.; Burris, H. A. A first-in-human phase I dose-escalation, pharmacokinetic, and pharmacodynamic evaluation of intravenous LY2090314, a glycogen synthase kinase 3 inhibitor, administered in combination with pemetrexed and carboplatin. *Invest. New Drugs* **2015**, *33*, 1187–1196.
- (29) Gentles, R. G.; Hu, S.; Dubowchik, G. M. Recent Advances in the Discovery of GSK-3 Inhibitors and a Perspective on their Utility for the Treatment of Alzheimer's Disease. *Annu. Rep. Med. Chem.* **2009**, *44*, 3–26.
- (30) Kramer, T.; Schmidt, B.; Lo Monte, F. Small-Molecule Inhibitors of GSK-3: Structural Insights and Their Application to Alzheimer's Disease Models. *Int. J. Alzheimer's Dis.* **2012**, *2012*, 1–32.
- (31) Selenica, M. L.; Jensen, H. S.; Larsen, A. K.; Pedersen, M. L.; Helboe, L.; Leist, M.; Lotharius, J. Efficacy of small-molecule glycogen synthase kinase-3 inhibitors in the postnatal rat model of tau hyperphosphorylation. *Br. J. Pharmacol.* **2007**, *152*, 959–979.
- (32) Chen, P. C.; Gaisina, I. N.; El-Khodori, B. F.; Ramboz, S.; Makhortova, N. R.; Rubin, L. L.; Kozikowski, A. P. Identification of a Maleimide-Based Glycogen Synthase Kinase-3 (GSK-3) Inhibitor, BIP-135, That Prolongs the Median Survival Time of $\Delta 7$ SMA KO Mouse Model of Spinal Muscular Atrophy. *ACS Chem. Neurosci.* **2012**, *3*, 5–11.
- (33) Saitoh, M.; Kunitomo, J.; Kimura, E.; Iwashita, H.; Uno, Y.; Onishi, T.; Uchiyama, N.; Kawamoto, T.; Tanaka, T.; Mol, C. D.; Dougan, D. R.; Textor, G. P.; Snell, G. P.; Takizawa, M.; Itoh, F.; Kori, M. 2-[3-[4-(Alkylsulfinyl)phenyl]-1-benzofuran-5-yl]-5-methyl-1,3,4-oxadiazole Derivatives as Novel Inhibitors of Glycogen Synthase Kinase-3 β with Good Brain Permeability. *J. Med. Chem.* **2009**, *52*, 6270–6286.
- (34) Onishi, T.; Iwashita, H.; Uno, Y.; Kunitomo, J.; Saitoh, M.; Kimura, E.; Fujita, H.; Uchiyama, N.; Kori, M.; Takizawa, M. A novel glycogen synthase kinase-3 inhibitor 2-methyl-5-(3-{4-[(S)-methylsulfinyl]phenyl}-1-benzofuran-5-yl)-1,3,4-oxadiazole decreases tau phosphorylation and ameliorates cognitive deficits in a transgenic model of Alzheimer's disease. *J. Neurochem.* **2011**, *119*, 1330–1340.
- (35) Uno, Y.; Iwashita, H.; Tsukamoto, T.; Uchiyama, N.; Kawamoto, T.; Kori, M.; Nakanishi, A. Efficacy of a novel, orally active GSK-3 inhibitor 6-Methyl-N-[3-[[3-(1-methylethoxy)propyl] carbamoyl]-1H-pyrazol-4-yl]pyridine-3-carboxamide in tau transgenic mice. *Brain Res.* **2009**, *1296*, 148–163.
- (36) Lesuisse, D.; Tiraboschi, G.; Krick, A.; Abecassis, P.-Y.; Dutruc-Rosset, G.; Babin, D.; Halley, F.; Château, F.; Lachaud, S.; Chevalier, A.; Quarteronet, D.; Burgevin, M.-C.; Amara, C.; Bertrand, P.; Rooney, T. Design of potent and selective GSK3 β inhibitors with acceptable safety profile and pharmacokinetics. *Bioorg. Med. Chem. Lett.* **2010**, *20*, 2344–2349.
- (37) Coffman, K.; Brodney, M.; Cook, J.; Lanyon, L.; Pandit, J.; Sakya, S.; Schachter, J.; Tseng-Lovering, E.; Wessel, M. 6-Amino-4-(pyrimidin-4-yl)pyridones: Novel glycogen synthase kinase-3 β inhibitors. *Bioorg. Med. Chem. Lett.* **2011**, *21*, 1429–1433.
- (38) Berg, S.; Bergh, M.; Hellberg, S.; Hogdin, K.; Lo-Alfredsson, Y.; Soderman, P.; von Berg, S.; Weigelt, T.; Ormo, M.; Xue, Y.; Tucker, J.; Neelissen, J.; Jerning, E.; Nilsson, Y.; Bhat, R. Discovery of Novel Potent and Highly Selective Glycogen Synthase Kinase-3 β (GSK3 β) Inhibitors for Alzheimer's Disease: Design, Synthesis, and Characterization of Pyrazines. *J. Med. Chem.* **2012**, *55*, 9107–9119.
- (39) Han, X.; Sivaprakasam, P.; Civiello, R. L.; Jacutin-Porte, S.; Kish, K.; Pokross, M.; Lewis, H. A.; Ahmed, N.; Szapiel, N.; Newitt, J. A.; Baldwin, E. T.; Xiao, H.; Krause, C. M.; Park, H.; Nophsker, M.; Lippy, J. S.; Burton, C. R.; Langley, D. R.; Macor, J. E.; Dubowchik, G. M. Discovery of new acylaminopyridines as GSK-3 inhibitors by a structure guided in-depth exploration of chemical space around a pyrrolopyridinone core. *Bioorg. Med. Chem. Lett.* **2015**, *25*, 1856–1863.
- (40) Yin, J.; Buchwald, S. L. Pd-catalyzed intermolecular amidation of aryl halides: the discovery that xantphos can be trans-chelating in a palladium complex. *J. Am. Chem. Soc.* **2002**, *124*, 6043–6048.
- (41) See [Supporting Information](#) for details. Compounds 4 and 7 had GSK-3 β IC₅₀'s of 1.5 and 3.8 nM, respectively, in our assay. Their Ambit profiles are shown in the [Supporting Information](#).
- (42) The GSK-3 β protein was expressed and purified as described in ref 31. The X-ray crystal structures of compounds 15 and 18 were deposited in the Protein Data Bank with PDB IDs SF94 and SF95. See the [Supporting Information](#) for details.
- (43) Aoki, M.; Yokota, T.; Sugiura, I.; Sasaki, C.; Hasegawa, T.; Okumura, C.; Ishiguro, K.; Kohno, T.; Sugio, S.; Matsuzaki, T. Structural insight into nucleotide recognition in tau-protein kinase 1/ glycogen synthase kinase 3 beta. *Acta Crystallogr., Sect. D: Biol. Crystallogr.* **2004**, *60*, 439–46.
- (44) The PyMOL Molecular Graphics System, version 1.0r2; Schrödinger, LLC: New York.
- (45) Karaman, M. W.; Herrgard, S.; Treiber, D. K.; Gallant, P.; Atteridge, C. E.; Campbell, B. T.; Chan, K. W.; Ciceri, P.; Davis, M. I.; Edeen, P. T.; Faraoni, R.; Floyd, M.; Hunt, J. P.; Lockhart, D. J.; Milanov, Z. V.; Morrison, M. J.; Pallares, G.; Patel, H. K.; Pritchard, S.; Wodicka, L. M.; Zarrinkar, P. P. A quantitative analysis of kinase inhibitor selectivity. *Nat. Biotechnol.* **2008**, *26*, 127–132.
- (46) The following kinases tested in-house for compound 15 all have IC₅₀'s > 2 μ M: Aurora-B, BTK, CDK2, CK2A2, IRAK4, JAK2, JNK1-R, LCK, LG921, and TYK2 887; the following kinases tested in-house for compound 18 all have IC₅₀'s > 50 μ M except for those with numbers (μ M) given in parenthesis: ABLWT (4.8), CDK5/p25 (5.4), cKIT, IGF1R, mAurA, MK2, P38A, PDGFR β , PIM1 (3.1), PKC θ , RSK1, and SYK.
- (47) The following kinases tested in-house for compound 18 all have IC₅₀'s > 2 μ M: Aurora-B, BTK, CDK2, CK2A2, CK2A2B, CK1E, IKK2, IRAK4, JAK1 CAL, FMS, JAK1, JAK2, JAK3, JNK1-R, LCK, LG921, ROCK1, ROCK2mut, SRMS, TRKA CAL, TRKB CAL,

TYK2, and TYK2 887; the following kinases tested in-house for compound 18 all have IC_{50} 's $> 50 \mu M$ except for those with numbers (μM) given in parenthesis: ABLWT (13), ACK, CDK5/p25, cKIT, IGF1R, mAurA, MK2, P38A, PDGRb (36), PIM1, PKCth, RSK1, and SYK. The following kinases tested in-house for compound 29 all have IC_{50} 's $> 2 \mu M$ except for those with numbers (μM) given in parenthesis: Aurora-B, BTK, CDK2, CK2A2, CK2A2B, CK1D, CK1E, FMS, IRAK4, JAK1 CAL, JAK2,, JAK3, LCK, LG921 (1.9), ROCK1, ROCK2mut, STK33AD, SRMS, TRKA CAL, TRKB CAL, TYK2, TYK2 887, and ZAP70; the following kinases tested in-house for compound 29 all have IC_{50} 's $> 50 \mu M$ except for those with numbers (μM) given in parenthesis: ABLWT (19), ACK, CDK5/p25 (42), cKIT, CSK, IGF1R, MK2, P38A, PDGRb, PKCth, and SYK. The following kinases tested in-house for compound 33 all have IC_{50} 's $> 2 \mu M$ except for those with numbers (μM) given in parenthesis: Aurora-B, BTK, BMX, CDK2, CK2A1, CK2A2, CK2A1B, CK2A2B, CK1D, CK1E, FMS, IRAK1 (1.6), IRAK4, ITK, JAK2, JAK3, JNK1-R, LCK, LG921, LYNA, ROCK1, ROCK2mut, STK33AD, TEC, TNIK, TRKA CAL, TRKB CAL, TYK2, TYK2 887, and ZAP70; the following kinases tested in-house for compound 33 all have IC_{50} 's $> 50 \mu M$ except for those with numbers (μM) given in parenthesis: CDK5/p25 (42), cKIT, CSK, FYN, IGF1R, mAurA, MK2, MARK1, MARK2, MARK3, MARK4, P38A, PDGRb, PIM1, PKCTH, RSK1, SYK (42), TTBK1, and TTBK2. The Ambit heat map values for compounds 18, 29, and 33 are shown in the [Supporting Information](#) as well.

(48) *Glycogen Synthase Kinase 3 (GSK-3) and Its Inhibitors: Drug Discovery and Development*; Martínez, A., Castro, A., Medina, M., Eds.; Wiley-Interscience: Hoboken, NJ, 2006.

(49) Oddo, S.; Caccamo, A.; Shepherd, J. D.; Murphy, M. P.; Golde, T. E.; Kaye, R.; Metherate, R.; Mattson, M. P.; Akbari, Y.; LaFerla, F. M. Triple-transgenic model of Alzheimer's disease with plaques and tangles: intracellular Abeta and synaptic dysfunction. *Neuron* **2003**, *39*, 409–421.

(50) See the [Supporting Information](#) for detailed data.